REPORT DOCUMENTATION PAGE

Public Reporting burden for this collection of information is estimated to average 1 hour per response, including the time for reviewing instructions, searching existing data sources, gathering and maintaining the data needed, and completing and reviewing the collection of information. Send comment regarding this burden estimates or any other aspect of this collection of information, including suggestions for reducing this burden, to Washington Headquarters Services, Directorate for information Operations and Reports, 1215 Jefferson Davis Highway, Suite 1204, Arlington, VA 22202-4302, and to the Office of Management and Budget, Paperwork Reduction Project (0704-0188,) Washington, DC 20503.

1. AGENCY USE ONLY (Leave Blank)	2. REPORT DATE March 30, 2004	3. REPORT TYPE AND DATES COVERED ~~March 30, 2000 – March 30, 2004~~ 01 Jul 00 – 31 Dec 03

4. TITLE AND SUBTITLE Synthesis of Irregular Diffractive Optical Elements	5. FUNDING NUMBERS C: DAAD 19-00-1-0387

6. AUTHOR(S) Kevin J. Webb	

7. PERFORMING ORGANIZATION NAME(S) AND ADDRESS(ES) School of Electrical and Computer Engineering Purdue University West Lafayette, IN 47907-1285	8. PERFORMING ORGANIZATION REPORT NUMBER

9. SPONSORING / MONITORING AGENCY NAME(S) AND ADDRESS(ES) U. S. Army Research Office P.O. Box 12211 Research Triangle Park, NC 27709-2211	10. SPONSORING / MONITORING AGENCY REPORT NUMBER 38781.1- PH

11. SUPPLEMENTARY NOTES

The views, opinions and/or findings contained in this report are those of the author(s) and should not be construed as an official Department of the Army position, policy or decision, unless so designated by other documentation.

12 a. DISTRIBUTION / AVAILABILITY STATEMENT Approved for public release; distribution unlimited.	12 b. DISTRIBUTION CODE

13. ABSTRACT (Maximum 200 words)

The theory of irregular diffractive optical elements is being developed by means of optimization software that allows wavelength-scale geometries to be synthesized. Structures are being designed for mode conversion and filtering demonstrations using the developed software. Example structures will be fabricated using silicon-based materials and then tested using near-field optical microscopy. This work will lay the foundation for applications such as VCSEL mode control and compact wavelength division multiplexing elements.

14. SUBJECT TERMS Diffractive elements, near field, mode conversion, optimization			15. NUMBER OF PAGES 10
			16. PRICE CODE

17. SECURITY CLASSIFICATION OR REPORT UNCLASSIFIED	18. SECURITY CLASSIFICATION ON THIS PAGE UNCLASSIFIED	19. SECURITY CLASSIFICATION OF ABSTRACT UNCLASSIFIED	20. LIMITATION OF ABSTRACT UL

NSN 7540-01-280-5500

Synthesis of Irregular Diffractive Optical Elements

Kevin J. Webb

Research Assistants: Ming-Chuan Yang, Jia-Han Li and Hua-Tsai Chen

School of Electrical and Computer Engineering, Purdue University,

West Lafayette, Indiana 47907

Phone: 765-494-3373, FAX: 765-494-2706, Email: webb@purdue.edu

Abstract

Functional electromagnetic field transformers, having irregular scattering profiles achieved through optimization, can provide wavelength-dependent transformation characteristics unattainable with photonic bandgap structures. Synthesis software for both waveguide and free space elements has been developed. Scanning-electron-microscopy photos of fabricated optical waveguide structures using electron beam lithography and a lift-off process show that the resolution required for communication wavelengths can be achieved. A microwave demonstration has established the wavelength-dependent functionality. Upon development of the physics and the mathematical tools, potential applications include wavelength division multiplexing elements and laser cavity mode control.

1   Introduction

The control and manipulation of light is important in signal processing related to optical communication applications and in the achievement of source coherence. Thus far, the majority of effort to control and filter electromagnetic waves has relied on wave scatter in periodic systems. This view has led to the significant level of interest in periodic photonic crystals [1].

Periodic structures have been suggested to realize various waveguides [2, 3, 4]. In addition, applications in reflectors and filters [5, 6, 7] have been proposed, while maintaining the incident mode profile, which usually refers to the uniform plane wave or the fundamental mode of the corresponding waveguide. Mode converters have also been implemented with a large set of periodic and perturbative scatterers to change the transverse field distribution of the incident field [8], which manipulates the field between two higher order modes. However, the ability to achieve filtering functions while performing transverse mode transformation has not yet been fully explored. As we demonstrate, there are opportunities to modify scattering structures in an aperiodic fashion, thereby transforming the spatial field essentially without loss and achieving some rather surprising scattering characteristics. Our field transformation elements fall into two groups: scattering from finite irregular diffractive elements in unbounded space and mode transformation in irregular waveguide structures.

2   Scatterers in Unbounded Space

2.1   Synthesis

Finite, irregular scattering structures in free space are considered which are compatible with implementation using solid state fabrication techniques. Structures have been studied which perform power splitting and wavelength-dependent scattering functions. Implementation with fiber optic systems should be possible.

Two classes of two-dimensional structures with conducting scattering elements in free space have been studied. One has a series of layers with locally periodic strips on each layer, which can be implemented using standard processing techniques. The other is more general, with more degrees of freedom, and has irregular conductor domains defined by a pixel representation.

We have used the finite element method (FEM) with a radiation boundary condition to solve the forward problem, i.e., given and incident field and a scattering structure, to determine the scattered field [9]. The Matlab optimization function *fmincon* is used for the synthesis of the multi-layer scattering structures and the iterative direct binary search method is used for synthesizing the more general pixel-based structures [10].

We have found that a multi-resolution synthesis procedure, where coarse adjustments in the scattering geometry are followed by successively finer adjustments, is an important strategy in finding satisfactory solutions with acceptable computational effort. Achieving a good initial guess is also important for expedient solutions. To achieve a good initial guess for a particular application, we tested several structures by randomly choosing the size and position of scatterers, and then proceeded with synthesis using the best candidate.

2.2 Aperiodic Multi-Layer Scattering Structures

For the multi-layer scattering structure, each layer can have several scatterers, and up to ten layers have been used. We used the Matlab *fmincon* continuous optimization routine applied to a locally periodic system of strips on each layer. The variables for each layer are then offset, period, duty cycle, and number of periods. The steps for strip width and layer spacing were reduced in later stages of the synthesis, thereby achieving a coarse to fine multi-resolution strategy. We achieved a wavelength-scale multi-layer structure which functions as a power divider. Figure 1 shows the case of a normally incident plane wave from above and two focal points just one wavelength below the structure.
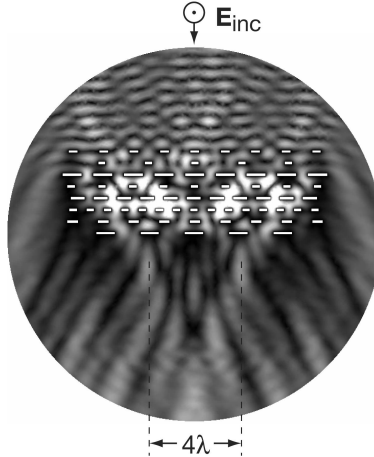

Figure 1: The amplitude of the total electric field for an 8-layer scattering structure which acts as a power divider. The focal plane is only one wavelength below the structure.

2.3 General 2-D Scattering Structures

We represent the general 2-D scattering structure by pixels, with each pixel being a scatterer (a conductor in this case) or not (free space in this case). Using discrete optimization, with an iterative

direct binary search method, a compact scattering structure with a wavelength-dependent transformation function has been found, as shown in Figure 2. The diffractive elements are conductors and the incoming plane waves have wavelength λ and 1.1 λ. The λ plane wave is focused on the left side, as shown in Figure 2(a), and the 1.1 λ plane wave is focused on the right side, as shown in Figure 2(b). The focal plane is located only 3 λ below the structure. Figure 2(c) shows the field amplitude squared of the λ and 1.1 λ waves at the focal plane, clearly showing the wavelength-dependent focal points and suggesting wavelength division multiplexing (WDM) applications. This example shows that irregular sub-wavelength scattering structures have the potential to achieve important functionalities with small size (just a few wavelengths on a side).
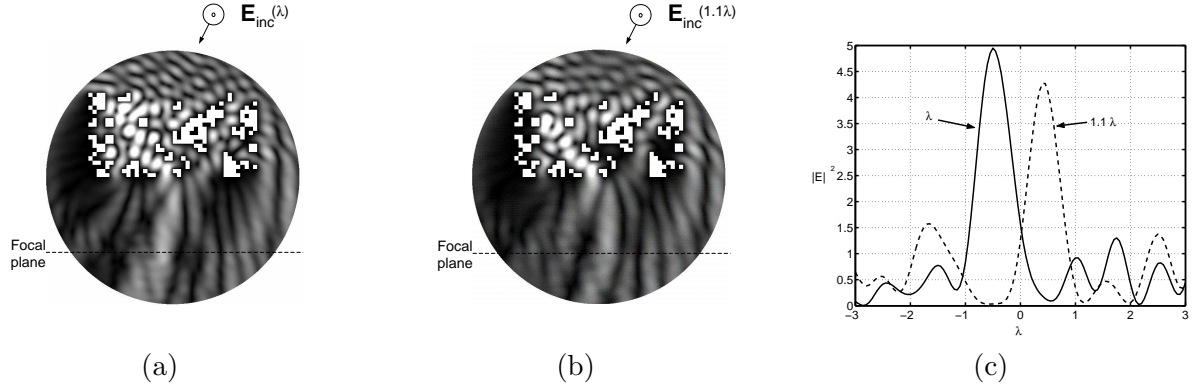

| (a) | (b) | (c) |

Figure 2: (a) Field amplitude pattern for the λ plane wave in structure performing a WDM function. (b) Field amplitude pattern for the 1.1 λ plane wave. (c) Field amplitude squared in the focal plane for the λ and the 1.1 λ plane waves.

3   Irregular Waveguide Structures

3.1   Synthesis

A schematic diagram of the uniform height, irregular width waveguide structure is shown in Fig. 3. Step-wise width variations introduce strong scatter. A generalized scattering matrix method using a modal expansion to match the fields between sections was used to solve the scattering behavior. Because each section offers two parameters, length and width, the number of degrees of freedom is therefore proportional to the number of sections. Synthesis was achieved using a multi-resolution algorithm which is an effective means for optimizing from a coarse model to a finer one.

3.2   Functionality

We have found several remarkable functionalities for field transformation in waveguide structures, as shown in Figure 4. Figure 4(a) shows a frequency-dependent transformation which converts the incident TE_{10} mode to the output TE_{30} mode at one frequency, but to the output TE_{10} mode at the other frequency. A wavelength-division-multiplexing element may be possible based on such a transformation. Figure 4(b) shows a mode-selective transformation which achieves total reflection for the incident TE_{10} mode and complete transmission for the incident TE_{20} mode at the same frequency. We therefore introduce the capability to distinguish different modes in a resonant cavity, allowing the control of the spatial mode profile if such an element serves as a feedback component. Figure 4(c) shows a multi-mode transformation which combines the incident equal-power and in-phase TE_{10} and TE_{30} modes into the output TE_{10} mode. On the other hand, reciprocity ensures
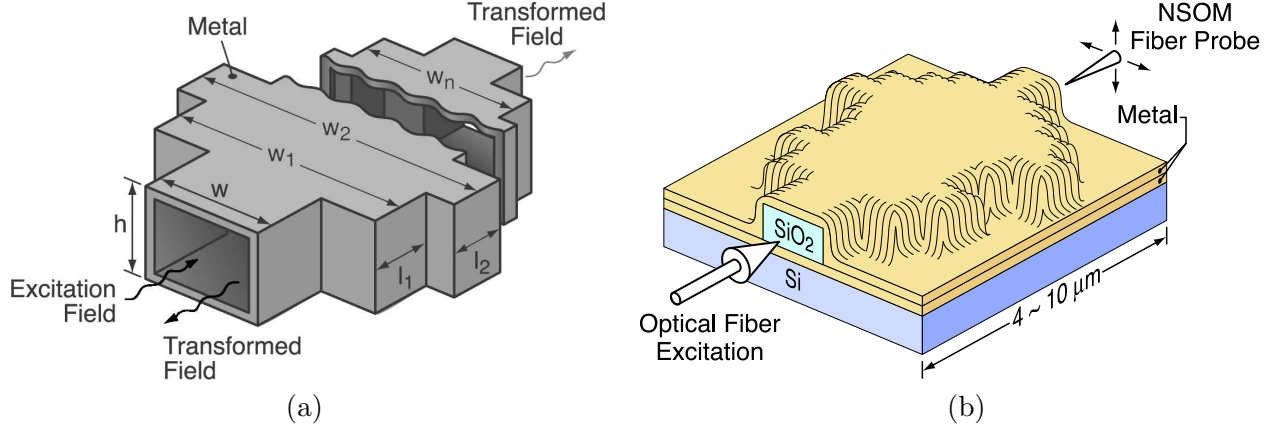
Figure 3: (a) Schematic diagram of a conducting wall waveguide field transformation element. The height of the waveguide is kept constant, while the width and length of each section are variable. (b) Proposed implementation.

that the incident TE_{10} mode from the output port will be split into TE_{10} and TE_{30} modes equally at the input port. This functionality shows the ability to control the content of the transformed mode, which is beyond the capability of the traditional one-to-one mode conversion. Figure 4(d) shows several elements to achieve different phase shifts relative to the incident plane. The elements are of the same length. Excitation of a phased-array antenna may be possible with such structures, providing a new solution for electronic beam steering.

We have found several solutions for all functionalities described, with each of them showing disparate spectral responses. This allows the selection of structures to achieve bandwidth control or synthesis based on spectral response.

3.3 Fabrication of Optical Devices

For optical communication wavelength implementation, resolution of the waveguide pattern requires 0.1 μm precision. The fabrication starts with a 100 ÅCr layer on a silicon substrate, followed by a 1000 ÅAu layer to form the bottom wall of the waveguide. The Cr layer is used to promote the adhesion between Si and Au. The wafer then undergoes an e-beam write on a bi-layer resist. After development of the resist, a 30 - 50 ÅCr layer is deposited, followed by a 0.1 μm thick layer of SiO_2. The Cr layer is used to promote the adhesion between oxide and Au. The waveguide pattern is formed after a lift-off process. The top and side metal walls of the waveguide are then formed by sputtering Ag on the wafer. In order to minimize the loss induced by the metal wall, only the neighborhood of the irregular waveguide region is covered by the sputtered Ag. The selective Ag deposition is achieved by photolithographically defining a window in the irregular waveguide region, Ag sputtering and then liftoff. The major challenge of this procedure lies in the e-beam direct write on the Au substrate, because there is significant back scattering of the electrons due to the large atomic number of Au, resulting in over-exposure. Careful calibration of the e-beam write is therefore required. Figure 5 shows two photos of test structures taken by scanning-electron-microscopy (SEM). Both structures are designed to perform TE_{10} to TE_{30} conversion at 1.55 μm. The dark background is the Au substrate and the lighter region is also Au, instead of SiO_2, which is used as a test procedure to demonstrate that the resolution requirement is met.
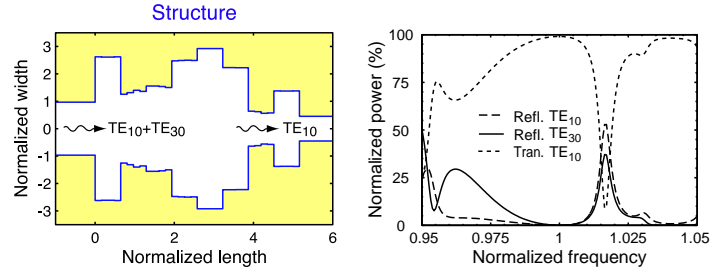
The waveguide elements will be tested by near field optical microscopy (NSOM) at the University
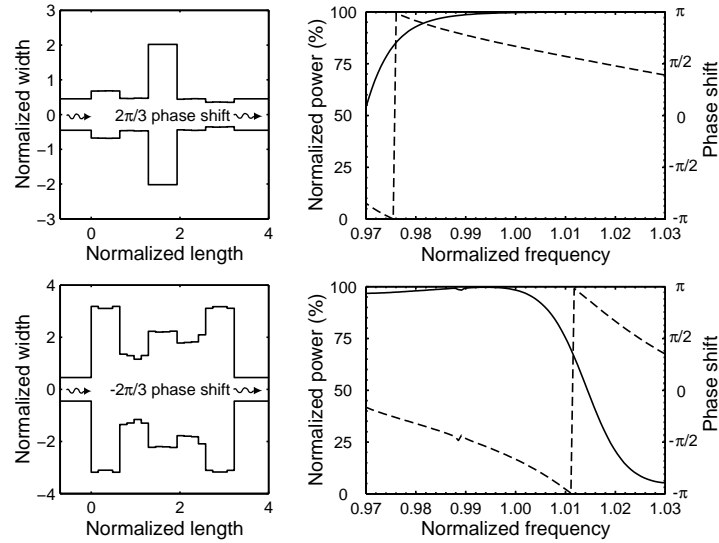
4
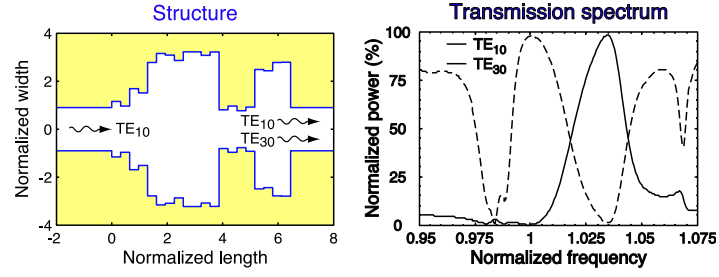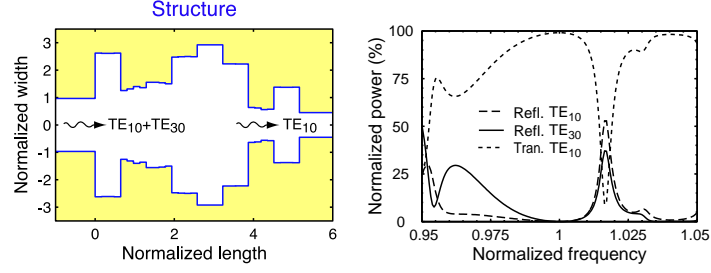
Figure 4: Functionalities of irregular waveguide structures. (a) Frequency-dependent transformation. (b) Mode-selective transformation. (c) Multi-mode transformation. (d) Phase shifters.
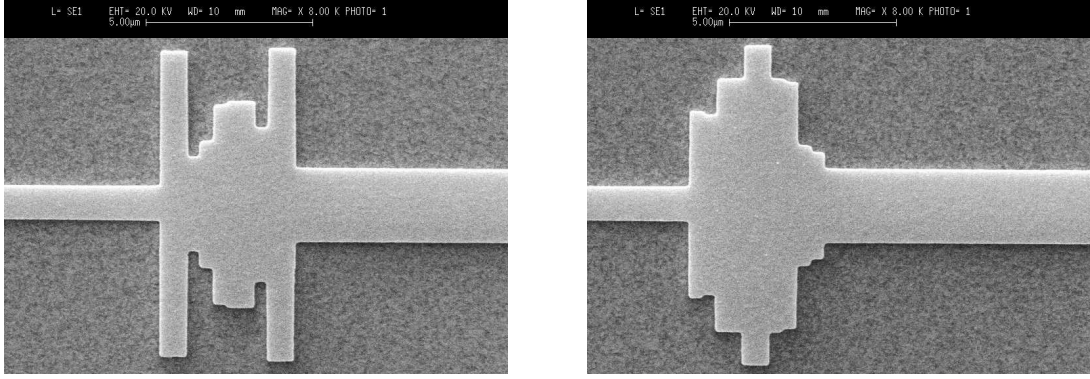
5

Figure 5: SEM photos of the fabricated irregular waveguide structures for TE_{10} to TE_{30} transformation at 1.55 μm. The input waveguide on the left is 1.0 μm wide and the output waveguide on the right is 2.1 μm wide. The 0.1 μm steps are clearly resolved.

of Illinois, Urbana (in collaboration with Prof. Chuang's group). The transformed field will be measured as a function of wavelength from 1.46 μm to 1.58 μm, and the results compared with simulations. The measured results will then be analyzed with a view to further refinement of the fabrication process.

3.4 Demonstration in the Microwave Frequency Range

To verify the field transformation functionality using an irregular waveguide structure, a frequency-dependent element was designed to operate at X-band and fabricated in brass. This element is to transform the incident TE_{10} mode to the output TE_{30} mode at 10 GHz, but to the output TE_{10} at 9.8 GHz. The resulting structure is shown in Fig. 6(a). Two slotted line measurements, one with a TE_{10} mode attenuator, allows the power in each of the two modes to be determined uniquely. The measured spectra are shown in Figs. 6(b) and (c). Good agreement is shown between the theoretical simulation and the experimental result, with a slight 30 MHz shift to higher frequency corresponding to 0.3% error at 10 GHz, within the tolerance of our mechanical fabrication. At the two frequencies where the complete transformation occurs, 9.8 GHz and 10 GHz, the reflection spectrum in Fig. 6(c) shows that almost no power is reflected, indicating that complete mode transformation is achieved.

4 Evanescent Fields in Left-Handed Materials

Negative refractive index or left-handed (LH) electromagnetic media [11] have received significant attention recently, both in terms of physical issues and also applications. One important suggestion was that it may be possible to build a perfect lens because of evanescent field growth with distance in a finite thickness slab [12] Interest accelerated after the experimental demonstration of a LH material at microwave frequencies [13]. To explore further the behavior of the evanescent field in LH material, we established the field solution for an electric current source at the interface between a positive refractive index and a negative refractive index medium using loss. Field growth and power dissipation relationships which we have derived provide metrics suitable for evaluating lens applications. Consequently, only a portion of the plane wave spectrum has the potential for growth to offset evanescent field decay between the object and image planes. However, the resulting
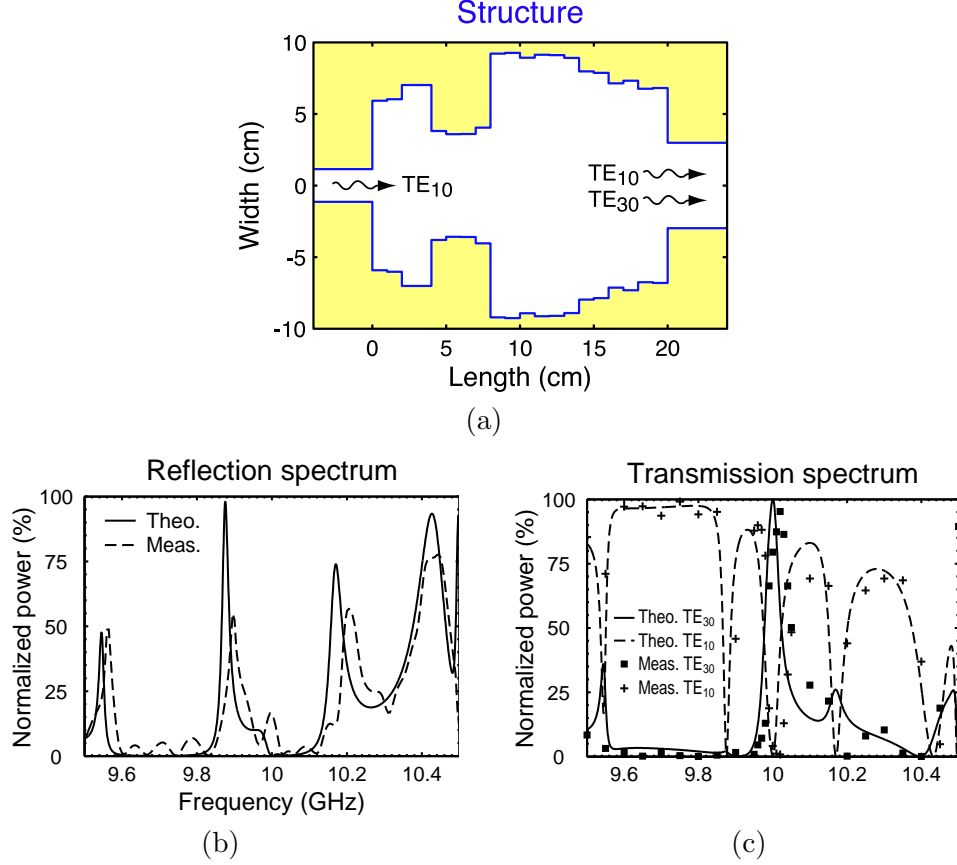
Figure 6: (a) Geometry of the frequency-dependent field transformation element. (b) The transmission spectrum of the TE_{30} and TE_{10} modes. Solid: simulation for TE_{30}; dashed: simulation for TE_{10}; squares: measured results for TE_{30}; diamonds: measured results for TE_{10}. (c) The reflection spectrum of the TE_{10} mode. Solid: simulation; dashed: measured results.

power dissipation suggests that these fields will be severely attenuated, making improved lensing problematic.

5   Plasmon Waveguides

It has been established that a chain of metallic nanoparticles (Au, for example) can guide light, thereby forming so-called plasmon waveguides [14, 15]. The guiding mechanism is linked with loss, i.e., closer field confinement to the nanoparticles requires higher loss (where field confinement is associated with guiding of the light). We studied both CdSe and Ag 2-D nanoparticle arrays using a finite element method, in order to investigate the wavelength and polarization dependence. The optical properties of bulk CdSe and Ag were used for the simulations [16, 17]. Figure 7(a) shows the simulation results for a CdSe chain with 20 cylinders having radius 15 nm and separation 15 nm, for TM polarization (the top two figures, where electric field is out of the page), and TE polarization (the bottom figure, where magnetic field is out of the page), at two wavelengths. Figure 7(b) uses the same sized structure as Fig. 7(a), but the cylinders are Ag. Effective guiding occurs in the Ag chain as the bulk plasmon resonance is approached, where the metal loss increases. Effective guiding in the Ag case occurs for TE polarization, whereas it is possible to guide both polarizations using CdSe.
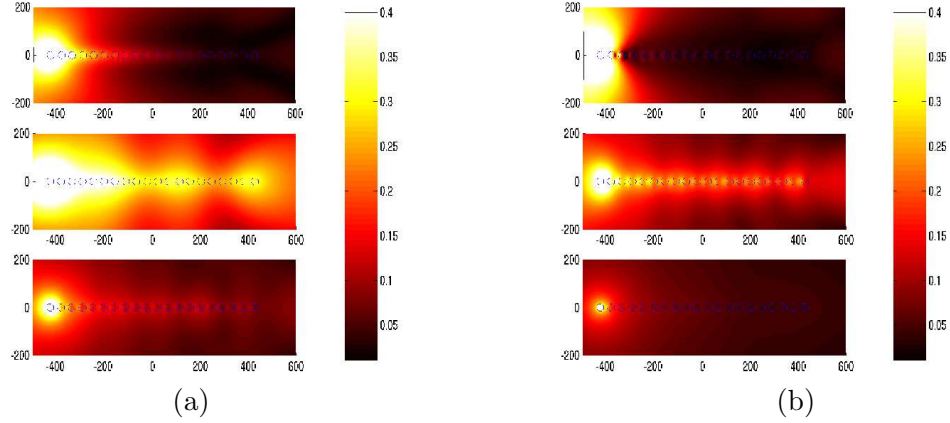
7

Figure 7: (a) Normalized field amplitudes for a chain of 20 CdSe cylinders in free space, with excitation at the left most cylinder. The cylinder radius is 15 nm and the separation between the cylinders is 15 nm. The top figure is the TM case with $\lambda = 350$ nm and $\epsilon_r = 7.087 - 4.283i$, the middle figure is the TM case with $\lambda = 701.4$ nm and $\epsilon_r = 7.854 - 1.294i$, and the bottom figure is the same as the top figure but for the TE case. (b) Normalized field amplitudes for a chain of 20 Ag cylinders in free space, with the left most cylinder excited. The cylinder radius is 15 nm and the separation is is 15 nm. The top figure is the TE case with $\lambda = 331.5$ nm and $\epsilon_r = -0.658 - 0.282i$, the middle figure is the TE case with $\lambda = 354.2$ nm and $\epsilon_r = -2.004 - 0.284i$, and the bottom figure is the TE case with $\lambda = 704.4$ nm and $\epsilon_r = -23.405 - 0.387i$.

6   Software

We have developed two synthesis codes, one for scattering structures in unbounded space and the other for waveguide structures. The coding to simulate the two-dimensional scattering in unbounded space is based on the finite element method and it is written using Matlab. We also have finite element code in Fortran for these problems that we have written (see [9]). The Partial Differential Equation and Optimization toolboxes in Matlab are used. The properties of the scattering structures and the incident wave can be chosen in the software package, and the multi-resolution method to synthesize the complex scatterers structure is also included in the software. For the waveguide structures, the electromagnetic solver is coded in C^{++} and compiled by the C^{++}-shell of Matlab, and serves as a normal Matlab function. The optimization script was coded in Matlab.

7   Publications

7.1   Journal Articles

1. K. J. Webb, M. Yang, D. W. Ward, and K. A. Nelson "Metrics for negative refractive index materials," *Phys. Rev. Lett.*, submitted.

2. M. Yang, J. Li, and K. J. Webb, "Functional field transformation with irregular waveguide structures," *Appl. Phys. Lett.*, **83**, 2736 (2003).

3. M. Yang, J. Li, and K. J. Webb, "Functional waveguide mode transformers," *IEEE Trans. Microwave Theory Tech.*, **52**, 161 (2004).

7.2 Conference Papers

1. M. Yang, J. Li, H. Chen, K. J. Webb (Purdue University), and G. Cueva (University of Illinois) "Field transformation and phase control in μm-scale metallic waveguides," *OSA Annual Meeting: Frontiers in Optics 2004*, Rochester, New York, 2004, *submitted.*

2. M. Yang, J. Li, H. Chen, K. J. Webb (Purdue University), P. Kondratko, S. L. Chuang, and G. Cueva (University of Illinois) "Near-field diffractive waveguide elements," *Annual APS March Meeting 2004*, Montreal, Quebec, Canada, 2003.

3. D. W. Ward, E. Statz, M. Yang, K. A. Nelson, and K. J. Webb (*Invited Speaker*) "Imaging and waveguide elements with periodic or negative refractive index materials," *Progress in Electromagnetics Research Symposium*, Honolulu, Hawaii, 2003.

4. K. J. Webb, M. Yang, J. Li, and H. Chen, "Near-field functional field transformation structures," *IEEE/OSA/APS Conf. Lasers and Electro-Optics*, Baltimore, MA, 2003.

5. M. Yang, J. Li, H. Chen, and K. J. Webb, "Near-field functional waveguide mode converter," *OSA Conf. Lasers and Electro-Optics/Pacific Rim*, Taipei, Taiwan, 2003.

6. M. Yang, J. Li, H. Chen, and K. J. Webb, "Wavelength-scale rectangular waveguide field transformation realization," *OSA Annual Meeting*, Orlando, FL, 2002.

7. J. Li and K. J. Webb, "Synthesis of multilayer aperiodic scattering structures," *IEEE APS/URSI Symp.*, San Antonio, TX, 2002.

8. K. J. Webb, M. Yang, J. Li, and H. Chen, "Field transformation in irregular waveguides," *Annual APS March Meeting*, Austin, TX, 2003.

9. M. Yang and K. J. Webb, "Synthesis of irregular waveguide field transformation elements using a multi-resolution algorithm," *IEEE APS/URSI Symp.*, San Antonio, TX, 2002.

10. M. Yang and K. J. Webb, "Functionality of optical field transformation in irregular waveguide structures," *IEEE/OSA/APS Conf. Lasers and Electro-Optics*, Long Beach, CA, 2002.

11. K. J. Webb, M. Yang, and J. Li, "Synthesis of irregular field transformation structures," *OSA Annual Meeting*, Long Beach, CA, 2001.

12. K. J. Webb, M. Yang and J. Li, "Synthesis and performance of irregular field transformation elements," *IEEE APS/URSI Symp.*, Boston, MA, 2001.

References

[1] E. Yablonovitch, "Inhibited spontaneous emission in solid-state physics and electronics," Phy. Rev. Lett. **58,** 2059–2062 (1987).

[2] Y. Fink, J. N. Winn, S. Fan, C. Chen, J. Michel, J. D. Joannopoulos, and E. L. Thomas, "A dielectric Omnidirectional Reflector," Science **282,** 1679–1682 (1998).

[3] S.-Y. Lin, E. Chow, V. Hietala, P. R. Villeneuve, and J. D. Joannopoulos, "Experimental demonstration of guiding and bending of electromagnetic waves in a photonic crystal," Science **282,** 274–276 (1998).

[4] J. C. Knight and P. S. J. Russell, "New ways to guide light," Science **296,** 276–277 (2002).

[5] D. C. Flanders, H. Kogelnik, R. V. Schmidt, and C. V. Shank, "Grating filters for thin film optical waveguides," Appl. Phys. Lett. **24,** 194–196 (1974).

[6] J. S. Foresi, P. R. Villeneuve, J. Ferrera, E. R. Thoen, G. Steinmeyer, S. Fan, J. D. Joannopoulos, L. C. Kimerling, H. I. Smith, and E. P. Ippen, "Photonic-bandgap microcavities in optical waveguides," Nature **390,** 143–145 (1997).

[7] D. J. Ripin, K.-Y. Lim, G. S. Petrich, P. R. Villeneuve, S. Fan, E. R. Thoen, J. D. Joannopoulos, E. P. Ippen, and L. A. Kolodziejski, "One-dimensional photonic bandgap microcavities for strong optical confinement in GaAs and GaAs/AlxOy semiconductor waveguides," J. Lightwave Technol. **17,** 2152–2160 (1999).

[8] J. S. Levine, "Rippled wall mode converters for circular waveguide," Int. J. Infrared and Millimeter Waves **5,** 937–952 (1984).

[9] B. Lichtenberg, K. J. Webb, D. B. Meade, and A. F. Peterson, "Comparison of two-dimensional radiation boundary conditions," Electromagnetics **16,** 359–384 (1996).

[10] D. J. Lieberman and J. P. Allebach, "A dual interpretation for direct binary search and its implications for tone reproduction and texture quality," IEEE Trans. Image Processing **9,** 1950–1963 (2000).

[11] V. G. Veselago, "The electrodynamics of substances with simultaneously negative values of ϵ and μ," Sov. Phys. Uspekhi **10,** 509–514 (1968).

[12] J. B. Pendry, "Negative refraction makes a perfect lens," Phys. Rev. Lett. **85,** 3966–3969 (2000).

[13] R. A. Shelby, D. R. Smith, and S. Schultz, "Experimental verification of a negative index of refraction," Science **292,** 77–79 (2001).

[14] S. A. Maier, P. G. Kik, and H. A. Atwater, "Observation of coupled plasmon-polariton modes in Au nanoparticle chain waveguides of different lengths: Estimatin of waveguide loss," Appl. Phys. Lett. **81,** 1714–1716 (2002).

[15] S. A. Maier, P. G. Kik, and H. A. Atwater, "Optical pulse propagation in metal nanoparticle chain waveguides," Phys. Rev. B 67 (2003).

[16] C. A. Leatherdale, W. K. Woo, F. V. Mikulec, and M. G. Bawendi, "On the abosrption cross section of CdSe nanocrystal quantum dots," J. Phys. Chem. B **106,** 7619–7622 (2002).

[17] P. B. Johnson and R. W. Christy, "Optical constant of the noble metals," Phys. Rev. Lett. **6,** 4370–4379 (1972).